Shape memory effects in melt-spun Fe–Mn–Si alloys

P. DONNER, E. HORNBOGEN, M. SADE*
Institut für Werkstoffe, Ruhr-Universität Bochum, D-4630 Bochum 1, FRG

There are three ways to produce shape memory alloys: (a) conventional melting and subsequent plastic deformation such as rolling and wire drawing; (b) pulver metallurgy; and (c) production of ribbons and wires by melt-spinning.

The third method is still at an exploratory stage. Earlier experiments with copper-based alloys as well as NiTi-base alloys have shown, however, that this method may lead to favourable shape memory properties [1, 2].

The advantage of this method can be threefold. (a) The concentration range in which a homogeneous high-temperature phase can be obtained is extended. (b) A favourable microstructure (columnar grains) and solidification texture can be achieved. (c) The semi-finished product (ribbon or wire) can be produced in a one-step procedure.

It is known from the theory of solidification that the formation of solid solutions from the liquid phase is generally associated with constitutional undercooling [3, 4]. This, in turn, leads to the formation of dendritic growth, which is associated with the local differences in chemical composition of the as-solidified crystalline structure. It is also known that the dendritic spacing decreases with the rate of solidification.

Recent work on rapid solidification from liquid has shown that at very high rates of solidification dendritic growth, and consequently segregation, disappears. In this case only one crystallization process, namely massive (or polymorphous) crystallization, takes place which leads to a solid solution of exactly the same chemical composition as the liquid from which it originated.

In addition to the known shape-memory alloys which have been mentioned above, iron-based alloys have attracted recent attention [5, 6]. It is the purpose of this work to explore the possibilities for melt-spinning of these alloys. In this context especially the as-solidified microstructure and its effect of the low-temperature phase transformation are the object of the investigation.

Thin ribbons were produced from bulk material. This is given in Table I. These ribbons were subsequently analysed by energy-dispersive X-ray analysis (EDAX), light and scanning electron microscopy. The data of the chemical analysis of the ribbons are also shown in Table I. The iron and manganese concentrations agree rather well with those of the original bulk material. The silicon shows a somewhat higher scatter, which could be partially due to inaccuracies of the chemical analysis.

TABLE I Chemical composition (mean values) of the alloys investigated. The analysis of the bulk material was compared with that of the melt-spun ribbons, which were made from the particular bulk material. The composition in both types of material agrees rather well. The scatter in silicon content may be due to inaccuracy in the chemical analysis of this element

Alloy	Nominal composition	EDAX bulk material (wt %)			EDAX melt-spun ribbons (wt %)		
		Fe	Mn	Si	Fe	Mn	Si
A	Fe–24Mn–3Si	72.7	24.3	3.0	71.4	24.2	4.4
B	Fe–26Mn–3Si	70.3	26.0	3.7	72.1	24.7	3.1
C	Fe–27Mn–3Si	69.3	27.3	3.4	71.9	25.6	2.5
D	Fe–28Mn–2Si	69.5	27.9	2.6	72.3	25.0	2.7
E	Fe–28Mn–3Si	69.0	27.8	3.2	68.9	26.8	4.3
F	Fe–30.5Mn–5Si	65.0	30.3	4.7	65.0	30.1	4.9
G	Fe–32Mn–4Si	64.1	32.0	3.9	64.2	32.2	3.6

Fig. 1 shows the metallographic analysis of cross-sections of alloy G, which were obtained from ribbons obtained with different surface velocities of the spinning wheel. A transition from coarser to finer dendritic growth to massive crystallization and formation of homogeneous grains becomes evident. Fig. 1d shows the as-solidified condition (e.g. of Fig. 1a) after a homogenization treatment in the solid state. Fig. 1c shows typical austenite grains at the onset of martensitic transformation. A volume fraction of 10 to 20% can be estimated. The amount of transformation in Fig. 1d is considerably larger. Quantitative evaluations from this microstructural analysis are shown in Fig. 2. The dendrite arm spacings decrease until between 30 and 40 m sec^{-1} the homogeneous phase forms directly from the liquid. The investigation with the Fe–Mn–Si alloys provided evidence for the whole range of phenomena between coarse dendrites and the homogeneous structure obtained by massive crystallization. Earlier investigations on copper and NiTi alloys only contained results on the situation shown on the right-hand side of this figure [7, 8].

The micrographs (Fig. 1) indicated that the martensite transformation starts somewhat above room temperature. This is corroborated by measurements of the transformation by differential scanning calorimetry (DSC; Fig. 3). These transformation temperatures agree rather well with those observed in earlier work on bulk material (Table II) [9].

The course of the transformation was observed by light microscopy and scanning electron microscopy (Fig. 4). The results confirm the well-known ⟨1 1 1⟩ fcc-habit of the transformation product. The observation that the individual growth of the martensite

*Humboldt-Fellow, on leave from Centro Atomico Bariloche, 8400 Bariloche, and CRUB, Universidad Nacional del Comahue, Argentina.

0261–8028/89 $03.00 + .12

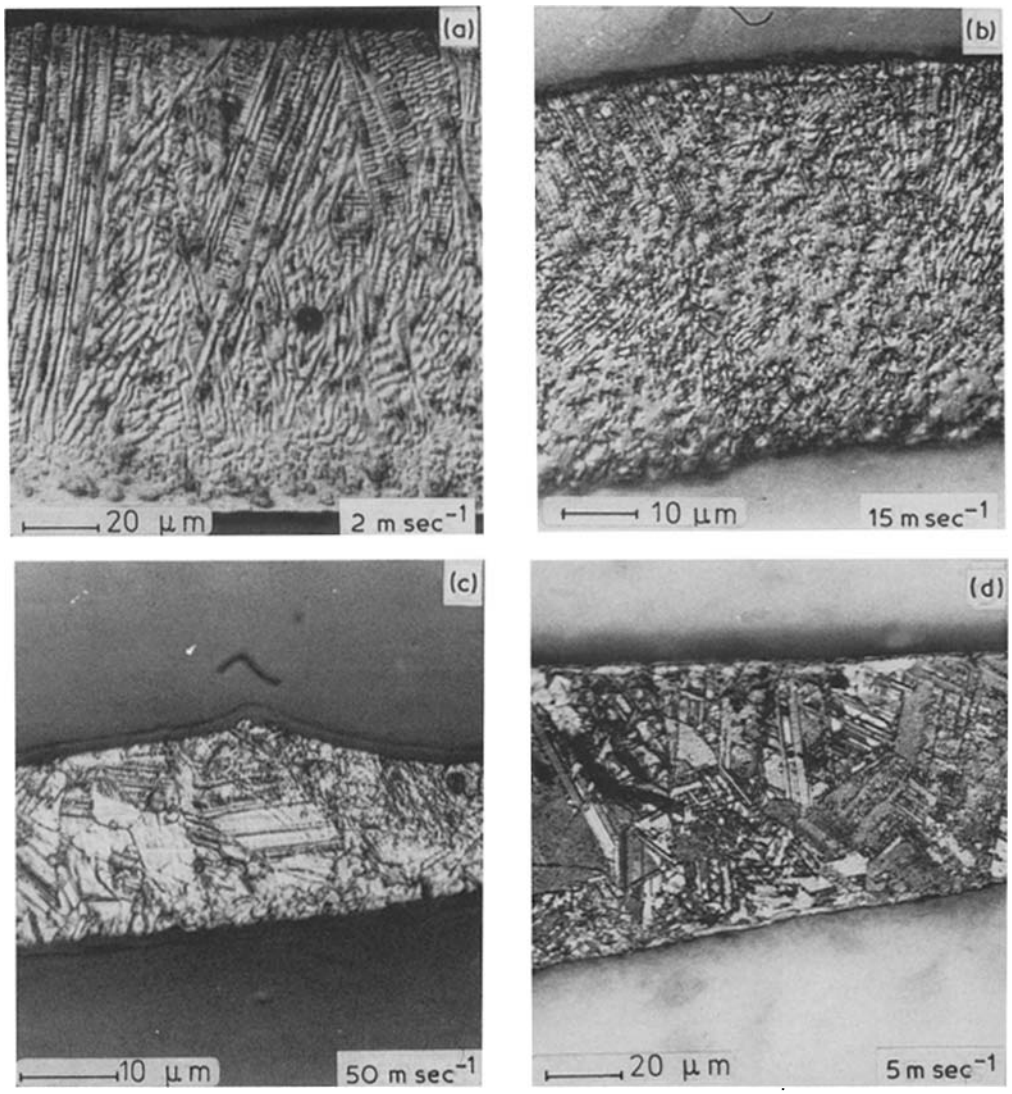

Figure 1 Light microscopy of cross-sections of melt-spun ribbons of alloy G. The wheel circumferential velocity is indicated. In (d) the alloy was treated at 1000° C (1 h) for rehomogenization. (c) and (d) show austenitic grains and partial martensitic transformation. (a) and (b) show the decreasing dendrite spacings, (c) and (d) provide evidence for the start of martensitic transformation in the homogeneous austenitic grains.

crystals is not stopped by the dendrites is remarkable. This provides evidence that the dendrites are completely coherent with the residual melt. The driving force for the martensitic transformation seems to vary little with local changes in composition due to the dendritic segregation.

From the metallographic investigation it could also be shown that $< 50\%$ is transformed. M_f is defined as the temperature at which no further transformation with additional undercooling is observed.

A conclusion of the suitability of the particular microstructures for shape memory is that thicker

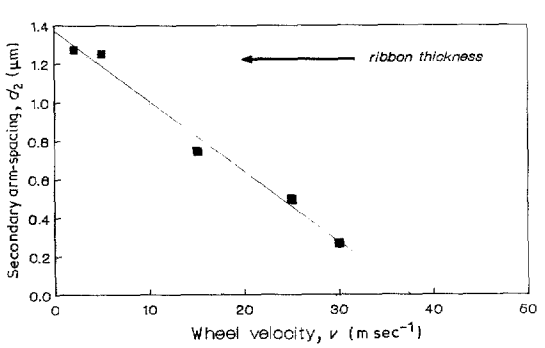

Figure 2 Quantitative evaluations of the microstructures obtained by different wheel velocities (i.e. cooling rates). Between 30 and 40 m sec^{-1} the massive crystallization reaction takes over and leads to a homogeneous γ-phase.

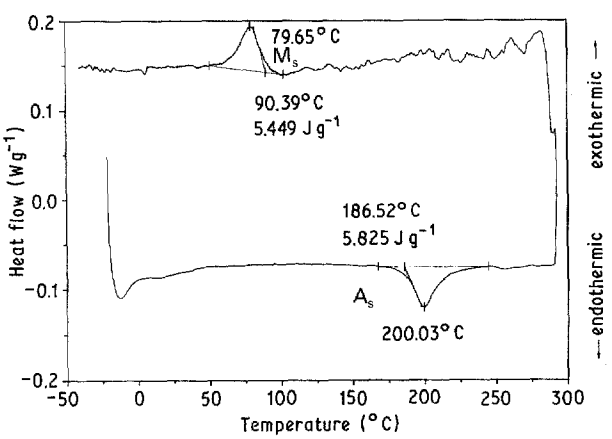

Figure 3 Typical results of the calorimetric measurements of the method of determining the start and finish of the transformation by DSC. For the evaluation of the heat of transformation the fraction of the high-temperature phase which is transforming would be required. It amounts to less than 50%. The accurate amount is still uncertain, therefore an accurate value for the heat of transformation cannot be obtained from this diagram.

TABLE II Typical transformation temperatures of the alloys in the different states as indicated. It should be noted that M_s is defined in the usual way (see Fig. 3). M_f is not the temperature of 100% transformation of austenite to martensite, but the temperature below which no further transformation takes place. The same is true for the reverse transformation. The transformation temperatures of the bulk material could be measured both by DSC and dilatometry, while calorimetry is one suitable method for the melt-spun alloys. The individual ribbons are not suitable for dilatometry.

Alloy	Temperature of bulk material (° C)				Temperature of as-quenched ribbon (° C)				Temperature of heat-treated ribbon (° C)			
	M_s	M_f	A_s	A_f	M_s	M_f	A_s	A_f	M_s	M_f	A_s	A_f
A	123	97	188	207	121	102	197	252	109	85	210	235
B	112	73	183	200	112	73	198	230				
B_{DSC}	117	73	176	218	112	73	198	230				
C	103	83	176	199	91	73	186	215	77	53	191	225
D	89	70	168	188	64	35	199	220	59	15	177	217
E	102	78	164	193	69	40	168	183	82	53	180	205
F	35	−3	154	178	37	5	155	193	43	1	158	184
G	25	−6	135	155	23	−3	128	158				

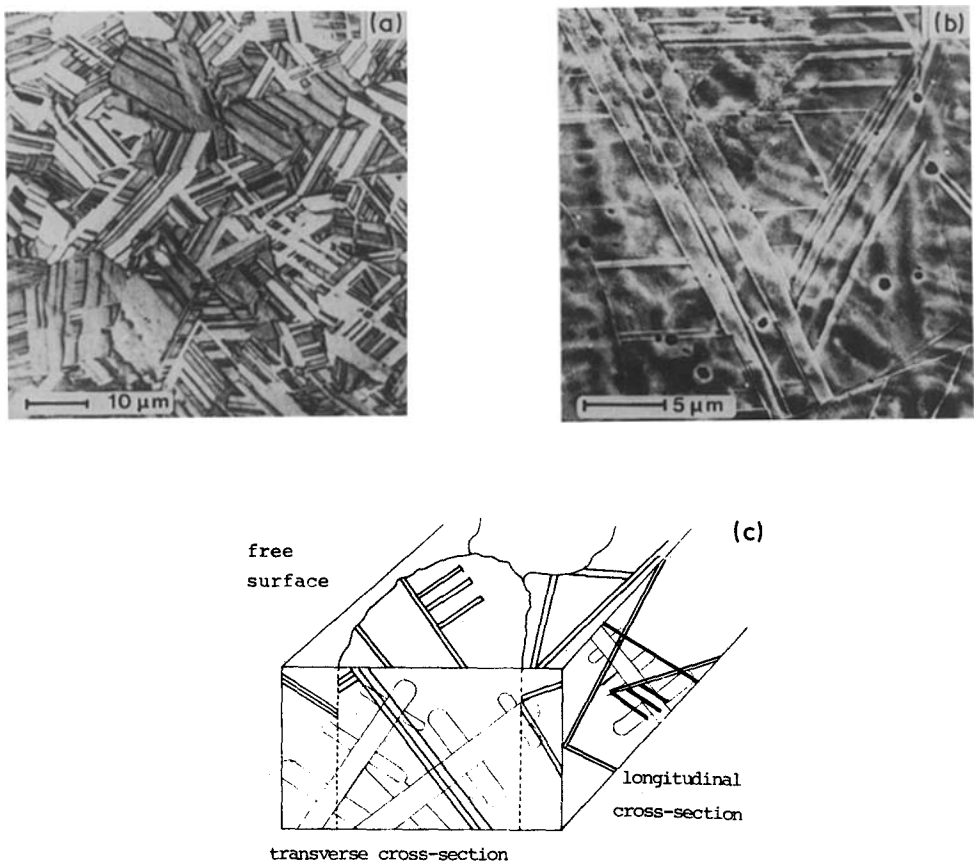

Figure 4 Light- and scanning electron micrographs of alloy F, showing the highest amount of transformation obtained by cooling far below M_f. The specimens were electrolytically polished. (b) shows the dendritic structure superimposed by the thin plates of martensites, which cut through the individual dendritic branches: (a) upper surface; (b) cross-section; and (c) schematic sketch which also indicates the planes of sectioning.

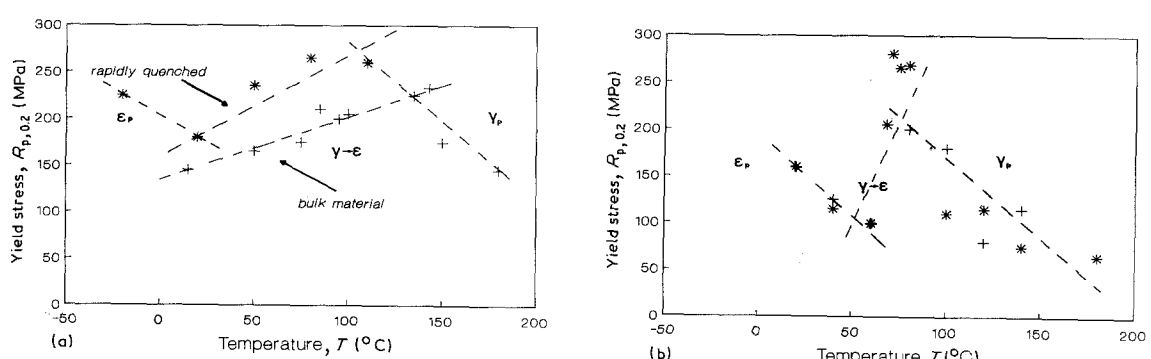

Figure 5 Results of tensile tests of bulk material and ribbons. The temperature ranges can be clearly distinguished. Plastic deformation of austenite, deformation to stress-induced $\gamma \rightarrow \varepsilon$ transformation and in the low-temperature range plastic deformation of martensite occurs. In addition, deformation of the residual austenite and minor amounts of strain-induced transformation might occur. (a) Fe–32.2Mn–3.6 Si, (b) Fe–30.1Mn–4.9 Si. (*) As quenched, (+) heat treated.

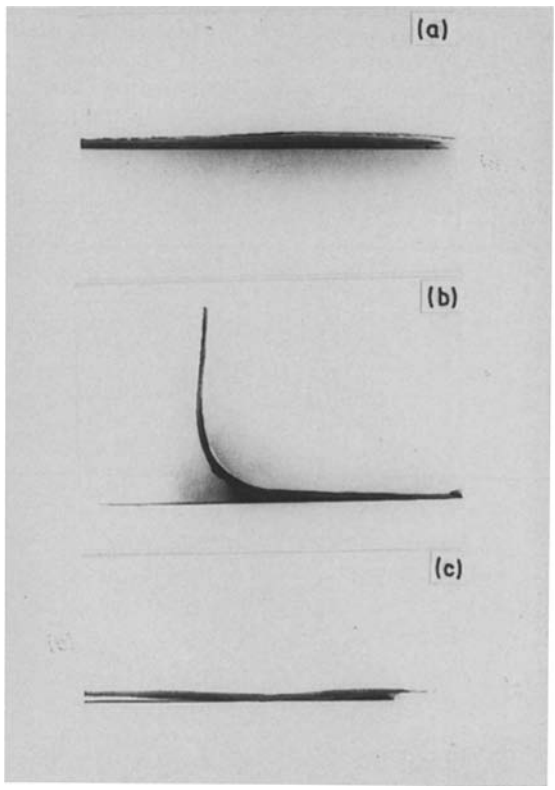

Figure 6 Qualitative deformation of the one-way effect, alloy F. (a) Initial state at room temperature; (b) bending deformation near the range of M_s (M_s = 37° C); and (c) after heating above A_f (about 200° C) a one-way effect of 100% could be observed. Ribbon thickness d = 160 μm.

ribbons containing dendrites may be used and that therefore the reheat treatment as shown in Fig. 1d does not seem to be necessarily required. This was confirmed by the measurements of mechanical properties which are shown in Figs 5a and b.

Figs 5a and b summarize some results of tensile tests conducted with the ribbons. The specimens were prepared from the ribbons by spark erosion. Figs 5a and b show the temperature dependence of the yield stress. Both alloys provide evidence for the anomalous drop of the yield stress in the region of M_s. After an increasing yield stress of the stable austenite, the yield stress starts to decrease as a consequence of the stress-induced $\gamma \rightarrow \varepsilon$ transformation. At low temperatures the yield stress increases again. Under these conditions no additional stress-induced transformation occurs and the temperature dependence of the untransforming phases becomes effective.

Figs 5a and b also indicate that there are no major differences between melt-spun and bulk material and the as-quenched and reheat-treated state. A major difference is a somewhat higher yield stress of the rapidly quenched alloys compared with the bulk material. This can be explained by a higher quenched-in defect density.

The alloys show an elongation at fracture of 5 to 6% in tensile tests. If this deformation is applied in the temperature range around M_s, then the one-way effect is observed (Fig. 6). In this case the bending deformation is completely recovered by reheating above A_f which, for this material, lies around 150° C. After an appropriate training a two-way effect is also observed in this alloy, which is, as usual, somewhat smaller than the one-way effect shown in Fig. 6.

Acknowledgements

The support of this work by the German Science Foundation (DFG Ho 325/21-1) is gratefully acknowledged. Thanks are also due to the Humboldt-Foundation, who provided for the research work of Dr M. Sade at the Ruhr-University.

References

1. S. EUCKEN and E. HORNBOGEN, in "Rapidly Quenched Metals", edited by S. Steeb and H. Warlimont (Elsevier Science, Amsterdam, 1985) p. 1429.
2. J. V. WOOD and W. M. STOBBS, in "Phase Transformations" (Institution of Metallurgists, York, 1979), p. IV 20.
3. B. CHALMERS, "Principles of Solidification" (Wiley, New York, 1964).
4. W. KURZ and D. J. FISHER, *Acta Metall.* **29** (1981) 11.
5. T. MAKI and I. TAMURA, in International Conference on Martensitic Transformations, Japan (1986) p. 963.
6. A. SATO and T. MORI, in Proceedings of the International Symposium on Shape Memory Alloys, Guilin, China, edited by C. Youyi, T. Y. Hsu and T. Ko (China Academic Publishers, 1986) p. 353.
7. S. EUCKEN and E. HORNBOGEN, "Strength of Metals and Alloys", edited by H. J. McQueen, J. P. Bailon, J. J. Dickson, J. J. Jonas and M. G. Akben (Pergamon Press, Oxford, 1985) p. 1779.
8. J. PERKINS, *Met. Trans.* **14A** (1983) 2229.
9. M. SADE, K. HALTER and E. HORNBOGEN, *J. Mater. Sci. Lett.* (1988) in press.

Received 3 May
and accepted 29 July 1988